28. Laviad, E. L., L. Albee, I. Pankova-Kholmyansky, S. Epstein, H. Park, A. H., Jr. Merrill, and A. H. Futerman. 2007. Characterization of ceramide synthase 2: Tissue distribution, substrate specificity and inhibition by sphingosine 1-phosphate. *J. Biol. Chem.* **283:** 5677-5684

29. Kihara, A., Y. Anada, and Y. Igarashi. 2006. Mouse sphingosine kinase isoforms SPHK1a and SPHK1b differ in enzymatic traits including stability, localization, modification, and oligomerization. *J. Biol. Chem.* **281:** 4532-4539

30. Bligh, E. G., and W. J. Dyer. 1959. A rapid method of total lipid extraction and purification. *Can. J. Med. Sci.* **37:** 911-917.

31. Han, X., and R. W. Gross. 2001. Quantitative analysis and molecular species fingerprinting of triacylglyceride molecular species directly from lipid extracts of biological samples by electrospray ionization tandem mass spectrometry. *Anal. Biochem.* **295:** 88-100

32. Ponec, M., A. Weerheim, P. Lankhorst, and P. Wertz. 2003. New acylceramide in native and reconstructed epidermis. *J. Invest. Dermatol.* **120:** 581-588

33. Rabionet, M., A. C. van der Spoel, C. C. Chuang, B. von Tumpling-Radosta, M. Litjens, D. Bouwmeester, C. C. Hellbusch, C. Korner, H. Wiegandt, K. Gorgas, F. M. Platt, H. J. Grone, and R. Sandhoff. 2008. Male germ cells require polyenoic sphingolipids with complex glycosylation for completion of meiosis: A link to ceramide synthase-3. *J. Biol. Chem.* in press

34. Brown, D. A., and E. London. 1998. Functions of lipid rafts in biological membranes. *Annu. Rev. Cell. Dev. Biol.* **14:** 111-136

35. Tojo, H. 2004. Properties of an electrospray emitter coated with material of low surface energy. *J. Chromatogr.* **A 1056:** 223-228

FIGURE LEGENDS

Fig. 1. Expression of *CerS3* mRNA is induced during differentiation of human keratinocytes. (A) Cultured human keratinocytes were differentiated for 0, 3, 6, or 9 days, and total RNA was prepared at each time point. RT-PCR was performed using primers specific for *FA2H*, *keratin 1* (a terminal differentiation marker), and *actin* (a loading control). PCR products were separated by 1.5% agarose gels and visualized. (B) Keratinocyte cDNA was prepared at each time point during differentiation. Real-time quantitative PCR was performed by the TaqMan method using primers and probes specific for *CerS1*, *CerS2*, *CerS3*, *CerS4*, *CerS5*, *CerS6*, and *18S ribosomal RNA* as a loading control. Values represent the mean ± SD of the amount of each *CerS* mRNA relative to that of the *18S ribosomal RNA* from three independent experiments.

Fig. 2. CerS family members produce 2-hydroxy-CER. (A) HEK 293T cells were transfected with pcDNA3 HA-1 (vector), pCE-puro 3xFLAG-FA2H (*FA2H*), or pCE-puro 3xFLAG-FA2H/pcDNA3 DES2 (*FA2H/DES2*), and labeled with 1 μCi [^{3}H]dihydro-Sph for 3 hr. Lipids were extracted, separated by TLC, and detected by X-ray film. The asterisk (*) indicates an unidentified band. (B) HEK 293T cells were transfected with pCE-puro 3xFLAG-FA2H (*FA2H*) together with pcDNA3 HA-1 (vector) or pcDNA3 HA-CerS3 (*CerS3*). Cells were untreated or treated with 20 μM FB_1 (a CER synthase inhibitor) then labeled and visualized as in (A). (C) HEK 293T cells were co-transfected with pCE-puro 3xFLAG-FA2H and pcDNA3 HA-1 (vector) or pcDNA3 HA-CerS3 (*CerS3*). Cells were harvested three days after transfection. Total lipids were extracted and hydrolyzed under mild alkaline conditions, and the

remaining sphingolipids were extracted by the Bligh and Dyer method. The fatty acid compositions of the total CER, including 2-hydroxy- and non-hydroxy fatty acids, were determined by HPLC/ion-trap mass spectrometry as described in "Materials and Methods". Each column is shaded to illustrate the total amounts of non-hydroxy CER (white) and 2-hydroxyl CER (black), relative to zero. (D) HEK 293T cells were co-transfected with pCE-puro 3xFLAG-FA2H and a *CerS*-encoding plasmid (pcDNA3 HA-CerS1 (*CerS1*), pcDNA3 HA-CerS2 (*CerS2*), pcDNA3 HA-CerS3 (*CerS3*), pcDNA3 HA-CerS4 (*CerS4*), pcDNA3 HA-CerS5 (*CerS5*), or pcDNA3 HA-CerS6 (*CerS6*)). Cells were untreated or treated with 20 μM FB_1 (a CER synthase inhibitor) then labeled and visualized as in (A).

Fig. 3. CerS1 exhibits 2-hydroxy-C18:0-CER synthesis activity *in vitro*. (A) Total cell lysates (20 μg protein) prepared from HEK 293T cells transfected with pcDNA3 HA-1 (vector), pcDNA3 HA-CerS1 (*CerS1*) or pcDNA3 HA-CerS6 (*CerS6*) were incubated at 37°C for 15 min with 0.2 μCi [^{3}H]dihydro-Sph, 5 μM dihydro-Sph, and either a non-hydroxy-CoA (C14:0, C16:0, C18:0, or C20:0) or 2-hydroxy-18:0-CoA (each at 25 μM). Lipids were extracted, separated by TLC, and detected by X-ray film. An asterisk (*) indicates an unidentified band. (B) Total cell lysates (100 μg protein) prepared from HEK 293T cells transfected with pcDNA3 HA-1 (control) or pcDNA3 HA-CerS1 (*CerS1*) were incubated at 37°C for 15 min with 5 μM dihydro-Sph, and 2-hydroxy-18:0-CoA. Lipids were extracted, directly separated on a normal-phase HPLC, and then monitored on-line with an LCQdeca-XP mass spectrometer via an

electrospray ion source. A fluoropolymer-coated electrospray ionization (ESI) tip (FortisTip, 20 μm ID and 150 μm OD, OmniSeparo-TJ, Hyogo) (35) was fit onto an xyz stage (AMR, Tokyo, JAPAN). Spectra in the positive and negative modes were alternately acquired by switching polarity at the ESI source on a single chromatographic run. (C) A mass spectrum near a peak at the retention time of 22.5 min on a chromatogram of *m/z*=584.7 ions (upper panel), a data-dependent MS/MS spectrum of *m/z*=584.7 ions (middle panel), and a successive MS/MS spectra of the *m/z*=566.4 ions formed by collision-induced dissociation (lower panel).

Fig. 4. CerS2 produces long-chain 2-hydroxy-CER and CerS5 short-chain 2-hydroxy-CER in HeLa cells overproducing FA2H. (A) Total RNA was prepared from HeLa cells and subjected to RT-PCR using primers specific for each *CerS* family member. PCR products were separated on 1.5% agarose gels and visualized. (B) HeLa cells were transfected with control siRNA, or siRNA specific for *CerS2* or *CerS5*. Three days after transfection, total RNA was prepared from each culture and subjected to RT-PCR using primers specific for *CerS2* or *CerS5*. *CerS4* and *actin* were used as loading controls. PCR products were separated on 1.5% agarose gels and visualized. (C) HeLa cells were co-transfected with pCE-puro 3xFLAG-FA2H (*FA2H*) and control siRNA (control) or siRNA specific for *CerS2* (*CerS2*), *CerS5* (*CerS5*), or *CerS2 and 5* (*CerS2, 5*). Three days after transfection, cells were labeled with 1 μCi [^{3}H]dihydro-Sph for 3 hr. Lipids were extracted, separated by TLC, and detected by autoradiography. The asterisk (*) indicates an unidentified band. (D) HeLa cells were co-transfected with

pCE-puro 3xFLAG-FA2H and control siRNA (c) or siRNA specific for *CerS2* (2), or *CerS5* (5). Cells were harvested three days after transfection, and total lipids were extracted then hydrolyzed under mild alkaline conditions, and the remaining sphingolipids were extracted by the Bligh and Dyer method. The fatty acid compositions of hexosyl CERs, including glucosyl and galactosyl CERs, were determined by HPLC/ion-trap mass spectrometry as described in "Materials and Methods". For each cell treatment, the column is shaded to illustrate the percentages of glucosyl CER (black) and galactosyl CER (white) present in either the non-hydroxy-hexosyl CER (upper panel) or 2-hydroxy-hexosyl CER (lower panel) lipid portion.

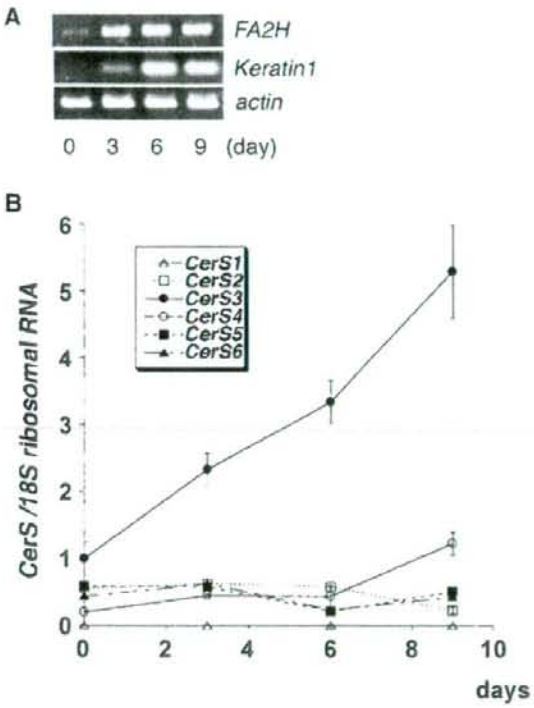

Fig. 1. Mizutani et al.

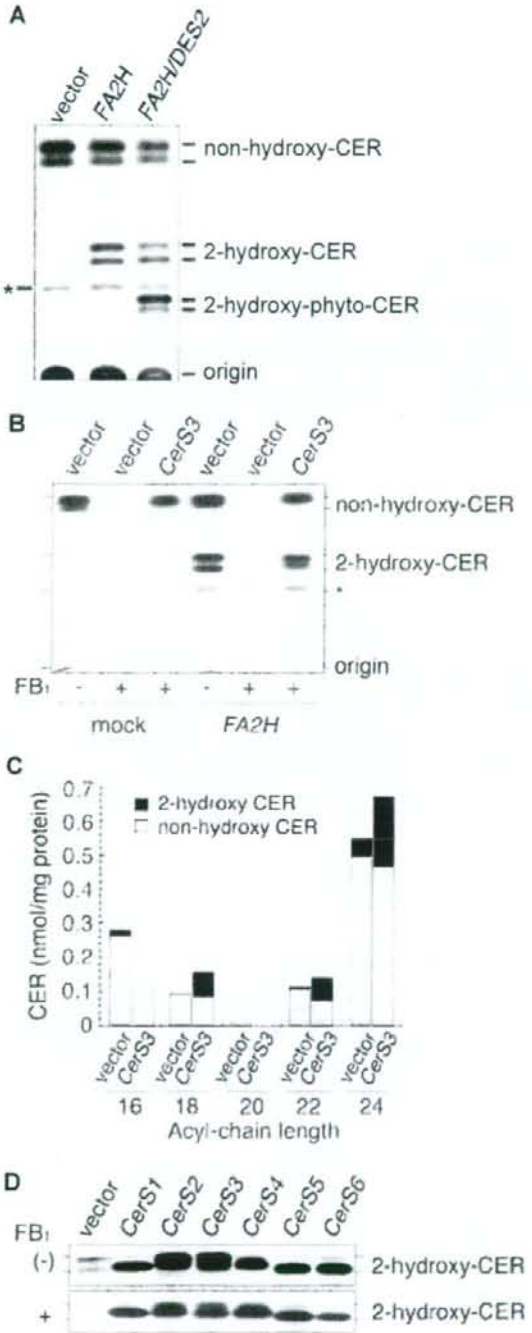

Fig. 2. Mizutani et al.

JOURNAL OF LIPID RESEARCH

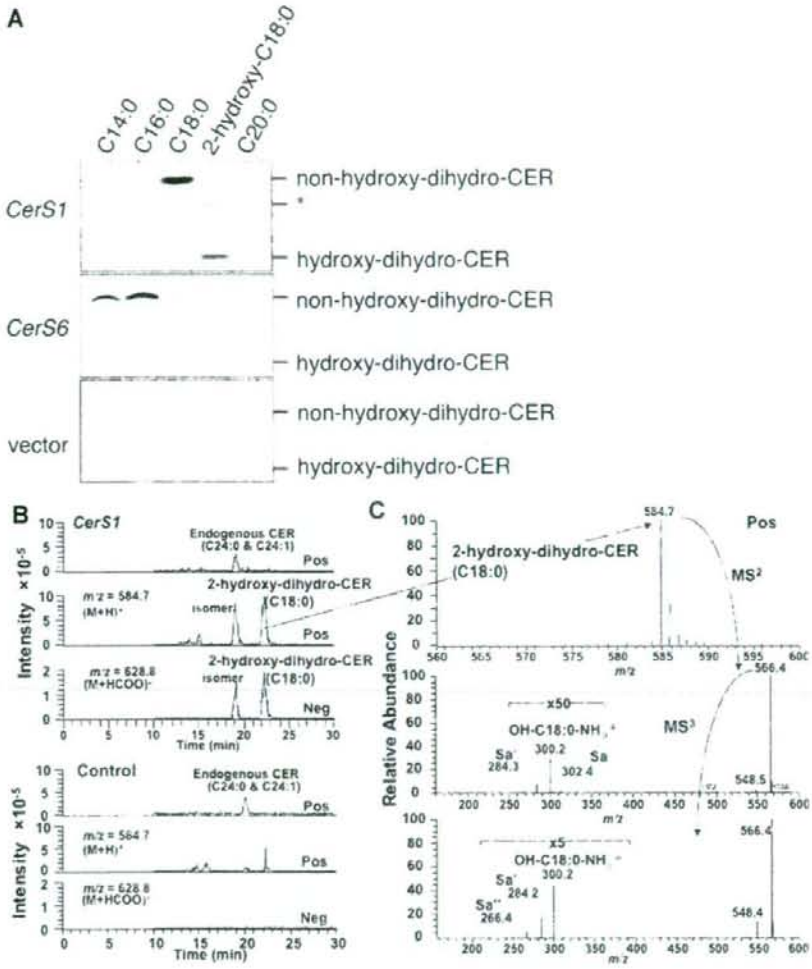

Fig. 3. Mizutani et al.

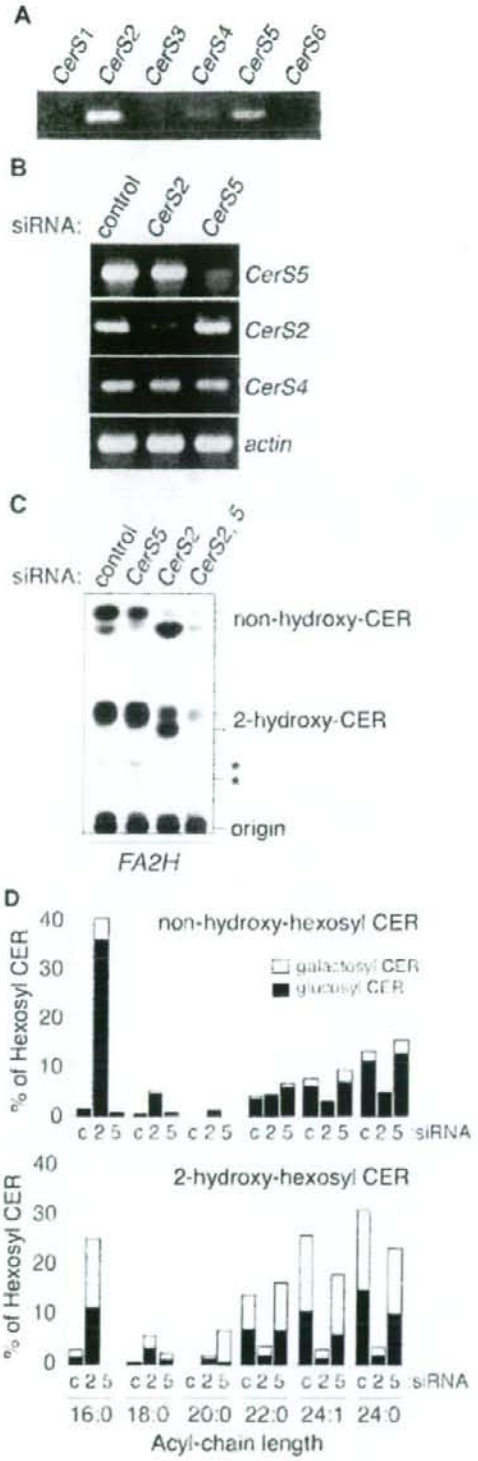

Fig. 4. Mizutani et al.

acteristically, a solitary subretinal granuloma is found either in the peripheral retina or macula or on the optic nerve.[1] Peripheral granulomas are the most common and are associated with the most visual morbidity because of tractional bands inciting cystoid macular edema (37.5%) or tractional retinal detachment (29.2%).[1] Other clinical presentations include vitritis (91.7%), retinal hemorrhage (20.1%), and optic disc swelling (16.7%).[1] Neovascularization of the disc and rubeosis are rare (4.2%).[1] Chronicity and recurrence of the disorder as seen in our patient may be related to a viable larvae within the eye, as has also been demonstrated in primate models, which have shown that in the quiescent form no larva is found.[3] The diagnosis of ocular toxocariasis is usually clinically based, as it may not be associated with eosinophilia or serum antitoxocara antibody positivity.[4] Thus, even when investigating exudative retinal detachment,[5] clinicians should be vigilant. In the literature, there are no reports of ocular toxocariasis with transvitreal migration or multiple granulomas as seen in our patient, who had two granulomas within the same eye.

Key Words: granuloma, intraocular larva, *Toxocara canis*, toxocariasis, transvitreal migration

Dhashani Sivaratnam, Visvaraja Subrayan, and Nadir A. Ali
Department of Ophthalmology, Faculty of Medicine, University of Malaya, Kuala Lumpur, Malaysia

Received: January 12, 2008 / Accepted: May 26, 2008
Correspondence to: Dhashani Sivaratnam, 124, Jalan Terasek 8, Bangsar Baru, Kuala Lumpur 59100, Malaysia
e-mail: Dhashani@hotmail.com

DOI 10.1007/s10384-008-0569-z

References

1. Stewart JM, Cubillan LD, Leo DP, et al. Prevalence, clinical features, and causes of vision loss among patients with ocular toxocariasis. Retina 2005;25:1005–1013.
2. Rodriguez A, Calonge M, Pedroza-Seres M, et al. Referral patterns of uveitis in a tertiary eye care center. Arch Ophthalmol 1996;114:593–599.
3. Watzke RC, Oaks JA, Folk JC. *Toxocara canis* infection of the eye. Correlation of clinical observations with developing pathology in the primate model. Arch Ophthalmol 1984;102:282–291.
4. Glickman LT, Schantz PM. Epidemiology and pathogenesis of zoonotic toxocariasis. Epidemiol Rev 1981;3:230–250.
5. Walton, David S, Mukai, et al. An 11-year-old girl with loss of vision in the right eye. N Engl J Med 2005;354:741–748.

Case of Aggressive Posterior Retinopathy of Prematurity with Atypical Neovascular Growth

Fibrovascular proliferation in eyes with retinopathy of prematurity (ROP) usually, but not always, appears at the junction of the vascularized and nonvascularized retina.[1] Aggressive posterior ROP (AP-ROP) occurs in the posterior retina and progresses rapidly to total retinal detachment.[2] We report an atypical case of AP-ROP in which the neovascularization developed in the posterior retina around the optic disc.

Case Report

A female infant was born at 30 weeks' gestation (birth weight, 1670 g) with severe persistent pulmonary hypertension from prolonged premature rupture of the membranes and oligohydramnios. She was treated with nitric oxide (NO) inhalation for 28 days. At 33 weeks postmenstrual age, an ophthalmoscopic examination identified initial signs of zone I AP-ROP bilaterally, including marked dilation and tortuosity of the posterior pole vessels (zone I, stage 1 ROP with plus disease).

Argon laser photocoagulation was performed (duration, 300–400 ms; power, 300–400 mW; 3751 shots OD, 3658 shots OS) under intravenous sedation (fentanyl) with topical anesthesia. However, fibrovascular proliferation and retinal detachment developed bilaterally in the posterior retina around the optic disc 1 week postoperatively (Fig. 1a, b). The patient underwent vitrectomy with lensectomy as a secondary treatment at 35 weeks postmenstrual age. The retina was reattached and the ROP stabilized in the left eye, but the fibrovascular tissue regrew from the posterior retina of the right eye (Fig. 1c). A second vitrectomy stabilized the ROP in that eye (Fig. 1d).

Immunohistochemistry of the fibrovascular tissue collected during vitrectomy was strongly positive for factor VIII over a wide area and locally positive for vimentin but negative for glial fibrillary acidic protein. These findings suggested that the tissue consisted mainly of vascular endothelial cells (Fig. 2).

Comments

We report the successful surgical results of early vitrectomy for AP-ROP.[3] Our findings suggest that when neovascularization develops only at the peripheral end of the developing vessels, the retina can be reattached by removing the vitreous framework around the fibrovascular tissue and the vitreous base. These procedures reduce the tractional forces of the fibrovascular tissue and suppress neovascular growth. Residual vitreous gel did not affect the retinal reattachment, and a regrowth of neovascularization was not observed in a previous study.[3]

In our case, the neovascularization that developed in the posterior retina could have grown along the residual vitreous gel on the retinal surface and around the optic disc. This tissue could not be completely removed during the initial vitrectomy. In cases such as this, another vitrectomy to peel the residual vitreous gel can lead to retinal reattachment, which worked well in our case.

Jpn J Ophthalmol
Vol 52: 407–425, 2008

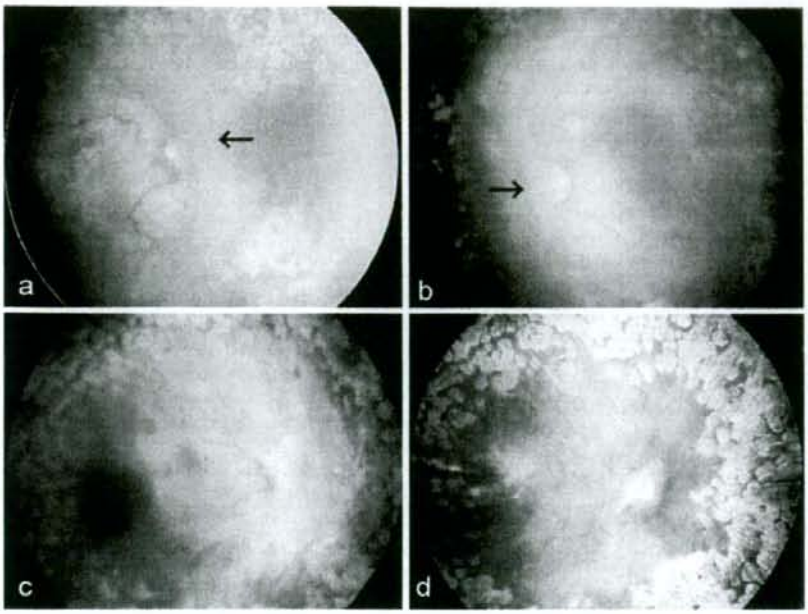

Figure 1a–d. Preoperative and postoperative fundus photographs of eyes with aggressive posterior retinopathy of prematurity (ROP). **a** Preoperative fundus image of the right eye. **b** Preoperative fundus image of the left eye. Fibrovascular proliferation and tractional retinal detachment (*arrows*) are present nasally in the posterior retina of both eyes. **c** Two weeks after the initial vitrectomy, the neovascularization has regrown and formed a fibrous membrane and tractional retinal detachment in the right eye. **d** The retina is reattached and the ROP is stabilized after additional vitrectomy of the right eye.

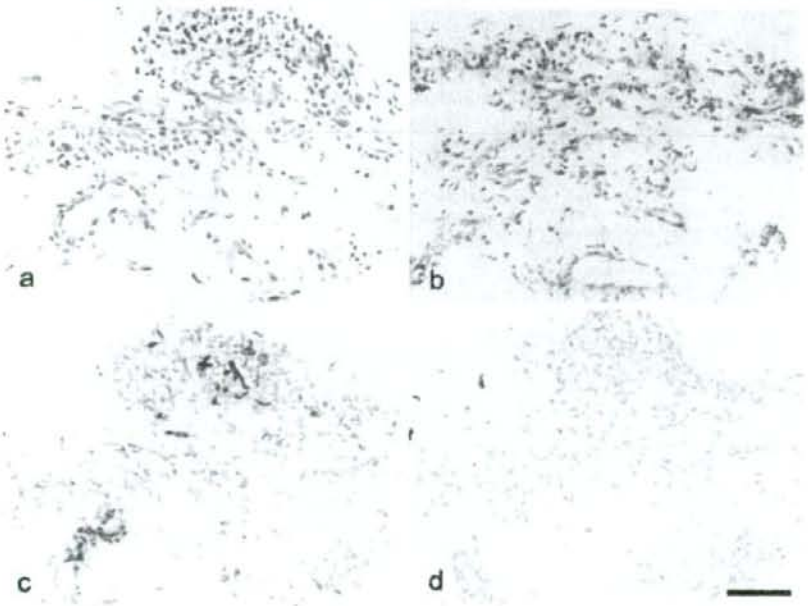

Figure 2a–d. Pathology and immunohistochemistry of the fibrovascular tissue obtained during the second vitrectomy. H&E staining (**a**) and immunohistochemistry with antibodies against factor VIII (**b**), vimentin (**c**), and glial fibrillary acidic protein (**d**). Immunohistochemistry showed that the fibrovascular tissue was strongly positive for factor VIII over a wide area (**b**), and was locally positive for vimentin (**c**) but negative for glial fibrillary acidic protein (**d**). These findings suggest that the tissue was composed of vascular endothelial cells (scale bar = 50 μm).

In eyes with AP-ROP, a flat network of neovascularization arises from the peripheral terminals of the developing vessels as in classical ROP, even though vascular shunts occur in the vascularized retina. However, in our patient, the fibrovascular proliferation developed atypically in the posterior retina around the optic disc. Except for the prolonged NO inhalation, systemic therapies including oxygen administration and laser application might not contribute

to the atypical growth of the neovascularization. While NO is known to derive vasodilatation and up-regulates regional basal blood flow,[4] it also activates angiogenic cell migration and proliferation-inducing factors, including fibroblast growth factor 2 and vascular endothelial growth factor.[5] Because retinal angiogenesis is ongoing in premature infants, NO might have contributed to the atypical neovascularization near the optic disc in our patient.

In animal models of oxygen-induced retinopathy, neovascularization induced by obliteration of the immature capillaries also develops from the optic disc and posterior retina.[6] Because AP-ROP develops in the posterior retinal area, including zone I, this suggests that immature capillaries may be widely present, and neovascularization arises from the retina near the optic disc. Capillary nonperfusion in vascularized retinas has been identified in eyes with threshold ROP.[7] Thus, there might be a much wider area of nonperfusion in the posterior retina in eyes with AP-ROP, which should be studied using fluorescein angiography.

Acknowledgments. This work was supported by grants for research on sensory disorders from the Ministry of Health, Labour and Welfare, Japan.

Key Words: aggressive posterior retinopathy of prematurity, fibrovascular proliferation, photocoagulation, regrowth, vitrectomy

Miina Hiraoka, Sachiko Nishina, Atsuko Nakagawa, Kentaro Matsuoka, and Noriyuki Azuma
Department of Ophthalmology, National Center for Child Health and Development, Tokyo, Japan

Received: December 11, 2007 / Accepted: April 23, 2008
Correspondence to: Noriyuki Azuma, Department of Ophthalmology, National Center for Child Health and Development, 2-10-1 Okura, Setagaya-ku, Tokyo 157-8535, Japan
e-mail: azuma-n@ncchd.go.jp

DOI 10.1007/s10384-008-0557-3

References

1. Foos RY. Retinopathy of prematurity. Pathologic correlation of clinical stages. Retina 1987;7:260–276.
2. International Committee for the Classification of Retinopathy of Prematurity. The international classification of retinopathy of prematurity revisited. Arch Ophthalmol 2005;123:991–999.
3. Azuma N, Ishikawa K, Hama Y, Hiraoka M, Suzuki Y, Nishina S. Early vitreous surgery for aggressive posterior retinopathy of prematurity. Am J Ophthalmol 2006;142:636–643.
4. Gross SS, Wolin MS. Nitric oxide: pathophysiological mechanisms. Annu Rev Physiol 1995;57:737–769.
5. Ziche M, Morbidelli L. Nitric oxide and angiogenesis. J Neurooncol 2000;50:139–148.
6. McLeod DS, D'Anna SA, Lutty GA. Clinical and histopathological features of canine oxygen-induced proliferative retinopathy. Invest Ophthalmol Vis Sci 1998;39:1918–1932.
7. Schulenburg WE, Tsanaktsidis G. Variations in the morphology of retinopathy of prematurity in extremely low birthweight infants. Br J Ophthalmol 2004;88:1500–1503.

Eyeball Luxation in *Bacillus cereus*-Induced Panophthalmitis Following a Double-Penetrating Ocular Injury

Since it was first reported in 1952, posttraumatic *Bacillus cereus* panophthalmitis has been known as a relatively rare but very serious progressive and devastating ocular infection usually leading to enucleation. The clinical features of this ocular infection include severe pain, chemosis, proptosis, and retinal hemorrhage.[1,2] In this report, we present a case that initially manifested as marked proptosis, then rapidly worsened into eyeball luxation at the time of surgery. To the best of our knowledge, ours is the first report of this unusual manifestation, which can be associated with double-penetrating ocular injury.

Case Report

A 30-year-old Japanese man visited our clinic with decreased vision and ocular pain. He recalled that about 14 h earlier his left eye might have been struck by a foreign body when he was trying to tie his shoestring while a truck was passing by. Unaware of the injury, he did not seek medical attention until the next morning, when he woke up with severe ocular pain. The patient's vision was reduced to uncertainty of light perception, the lids were swollen and ecchymotic, and the conjunctiva was severely chemotic (Fig. 1A). On slit-lamp examination the cornea was diffusely edematous, and a 3.5-mm corneal laceration was visible close to the temporal limbus. A severe fibrinous iritis and hypopyon were present, and fundus details could not be visualized. Computed tomography revealed the presence of an intraocular foreign body in the posterior vitreous (Fig. 1B). The patient received immediate anterior chamber and intravitreal injection with vancomycin (1 mg/0.1 ml) and imipenem (2 mg/0.1 ml). Within 2 h after admission, the proptosis of his left eye had rapidly worsened into eyeball luxation and complete ophthalmoplegia (Fig. 1C). At the time of surgery, leukocytosis and malaise were remarkable. His temperature rose to 38.7°C, and the white cell count was 21.1×10^3 and the C-reactive protein level was 10.30 mg/dl. Septicemia was suspected, and ocular enucleation was performed. Surgical findings revealed a scleral laceration 10 mm behind the temporal limbus, and a metallic foreign body measuring 4×2.5 mm was found in the prolapsed vitreous (Fig. 1D). Enucleation alone could not reduce the swollen orbital tissues, and partial tarsorrhaphy was performed to close the eyelids.

Postoperatively the patient became afebrile within 48 h, the swollen orbital tissues resolved, and he recovered uneventfully. Pathological examination of the enucleated eyeball demonstrated that there was intensive neutrophilic infiltration around the perforated sclera, and the sclera was found to be entirely melted (Fig. 2A and B). In addition, a

Graefes Arch Clin Exp Ophthalmol (2008) 246:453–455
DOI 10.1007/s00417-007-0741-z

CASE REPORT

Exudative retinal detachment following cataract surgery in Hallermann-Streiff syndrome

Sachiko Nishina · Yumi Suzuki · Noriyuki Azuma

Received: 7 September 2007 / Revised: 17 November 2007 / Accepted: 27 November 2007 / Published online: 12 January 2008

Abstract
Purpose To report two cases of Hallermann-Streiff syndrome with exudative retinal detachment after cataract surgery.
Methods Case report.
Results Four eyes of two patients with Hallermann-Streiff syndrome developed exudative retinal detachments after lensectomy and anterior vitrectomy at 2 and 4 months of age. Both patients had extreme microphthalmia. The exudative retinal detachment regressed spontaneously in three of the four eyes; however, one eye required subscleral sclerectomy. In one patient, the best-corrected visual acuity was 20/200 at 3 years of age; the other patient had good fixation and following behavior in each eye at 1 year of age.
Conclusions Early surgery to treat congenital cataracts in extremely microphthalmic eyes associated with the Hallermann-Streiff syndrome may induce exudative retinal detachment. However, the retinal detachments tend to regress and may not cause severe visual impairment.

Keywords Hallermann-Streiff syndrome · Exudative retinal detachment · Cataract surgery · Microphthalmos

Introduction

The Hallermann-Streiff syndrome is a rare complex of developmental abnormalities characterized by dyscephaly with bird face, beak nose and micrognathia, dental anomalies, hypotrichosis, skin atrophy, microphthalmia, congenital cataracts, and proportionate dwarfism [1]. Most cases are sporadic, and the etiology is unknown. Various ocular findings and fundus anomalies have been reported, including vitreous degeneration, retinal folds, coloboma, and Coats' disease; however, a few reports have described detailed fundus changes after cataract surgery [2–4]. To our knowledge, this is the first report on the development of exudative retinal detachments after cataract surgery in four microphthalmic eyes of two patients with the Hallermann-Streiff syndrome.

Case report

Patient 1, a 1-month-old Japanese male infant, referred with a diagnosis of bilateral congenital cataracts and microphthalmia. He had the typical features of the Hallermann-Streiff syndrome, including dyscephaly with beak nose and micrognathia, dental anomalies, hypotrichosis, skin atrophy, and proportionate dwarfism (Fig. 1a). A slit-lamp examination revealed total cataracts, a microcornea (corneal diameter, 7×7.5 mm OD and 8×8.5 mm OS), a shallow anterior chamber, posterior synechiae, and poor pupil dilation in both eyes. Ultrasonography showed bilateral microphthalmia (axial length, 13 mm OD and 14 mm OS) but no other posterior segment anomalies. Lensectomy and anterior vitrectomy via the limbal approach using a 25-gauge surgical system was performed in both eyes at 2 months of age. No intraoperative or postoperative complications developed except for transient corneal edema. Ophthalmoscopy identified small retinal folds between the disc and fovea in both eyes. The aphakic eyes were corrected with glasses, and both eyes developed fixation and following behavior.

The authors have no proprietary interest in any aspect of this report.

S. Nishina (✉) · Y. Suzuki · N. Azuma
Department of Ophthalmology,
National Center for Child Health and Development,
2-10-1 Ohkura, Setagaya-ku,
Tokyo 157-8535, Japan
e-mail: nishina-s@ncchd.go.jp

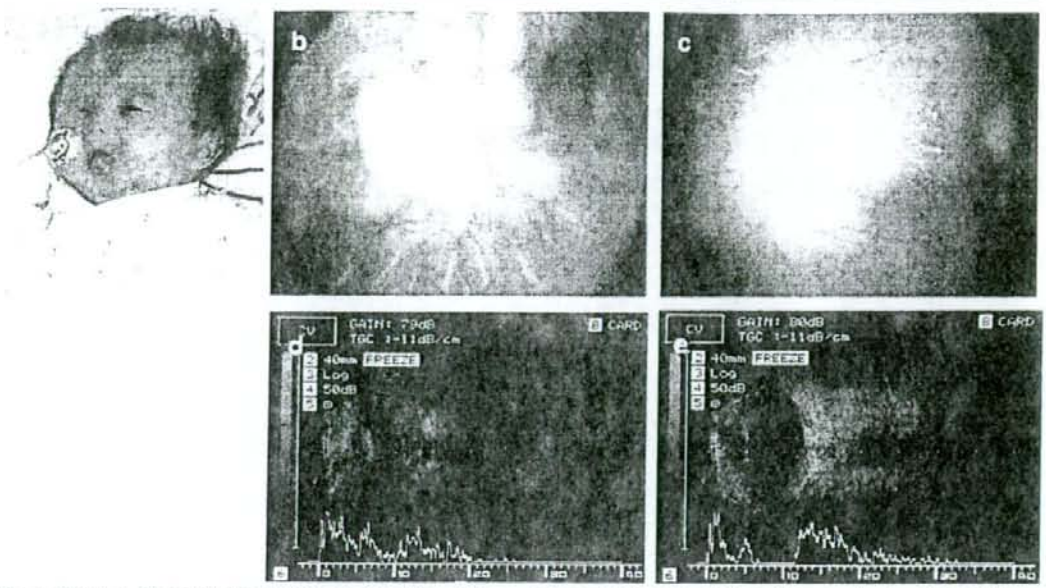

Fig. 1 Patient 1. (**a**) Facial characteristics at 2 months of age. Bilateral exudative retinal detachments at 7 months of age. The right eye (**b**) has the more severe retinal detachment and requires subscleral sclerectomy. The left eye (**c**) also has an exudative retinal detachment that regressed spontaneously. Ultrasonography shows both right eye (**d**) and left eye (**e**) have exudative retinal detachments with choroidal thickening

We examined the patient every month and then at 5 months after cataract surgery (7 months of age) when exudative retinal detachment developed in both eyes (Fig. 1b,c). Ultrasonography also showed bilateral exudative retinal detachment with choroidal thickening (Fig. 1d,e). The retinal detachment spontaneously regressed in the left eye, but progressed and did not regress in the right eye. Following behavior in the right eye deteriorated, and we performed a subscleral sclerectomy twice in that eye using 0.02% mitomycin C at 1 year 9 months and 2 years 4 months of age. The retinal detachment regressed, and at 3 years 5 months of age did not recur in either eye. The best-corrected visual acuity (BCVA) was 2/100 in the right eye and 20/200 in the left eye.

Patient 2, a 5-month-old Japanese female infant, referred with a diagnosis of bilateral retinal detachments after cataract surgery. She had undergone lensectomy and anterior vitrectomy at 4 months of age in another hospital. She exhibited the characteristic features of the Hallermann-Streiff syndrome, including dyscephaly with beak nose and micrognathia, dental anomalies, hypotrichosis, and proportionate dwarfism. A slit-lamp examination showed bilateral aphakia and a microcornea (corneal diameter, 7×7.5 mm OD and 8×8.5 mm OS). Ophthalmoscopy of both eyes showed exudative retinal detachments (Fig. 2). Ultrasonography showed bilateral microphthalmia (axial length, 13 mm OD and 14 mm OS) and retinal detachments with choroidal thickening. The retinal detachments spontaneous-

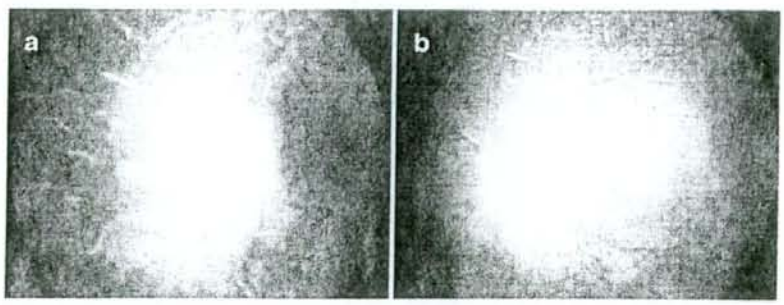

Fig. 2 Patient 2. Bilateral exudative retinal detachments at 1 years of age. The exudative retinal detachments regressed spontaneously in the right eye (**a**) and the left eye (**b**)

ly regressed in both eyes, and the patient had good fixation and following behavior with each eye at 1 year of age.

Discussion

These four eyes of two patients had severe microphthalmos and developed exudative retinal detachments after early surgery for congenital cataracts at 2 and 4 months of age. One of the four eyes required surgery; however, the retinal detachment regressed in three eyes, and the visual acuity was not severely impaired. This suggests that the extreme microphthalmic eye in the Hallermann-Streiff syndrome may have considerable scleral abnormalities that impede transscleral intraocular fluid outflow and result in congestion of the choroidal vein [5]. Early cataract surgery is supposed to induce hypotony, marked intraocular inflammation and transiently accelerate production of a protein-rich exudate. Intraocular fluid outflow may severely be resisted postoperatively and accumulated in choroid without venous drainage. It may possibly cause early onset of exudative retinal detachment in these eyes.

In this syndrome, spontaneous cataract absorption sometimes occurs, but results in deprivation amblyopia, iridocyclitis, and glaucoma [4, 6]. Although exudative retinal detachment tends to occur, it is preferable to perform early cataract surgery using less invasive procedures.

References

1. François J (1958) A new syndrome: Dyscephalia with bird face and dental anomalies, nanism, hypotrichosis, cutaneous atrophy, microphthalmia, and congenital cataract. Arch Ophthalmol 60:842–862
2. Cohen MM Jr (1991) Hallermann-Streiff syndrome: a review. Am J Med Genet 41:488–499
3. Newell SW, Hall BD, Anderson CW, Lim ES (1994) Hallermann-Streiff syndrome with Coats disease. J Pediatr Ophthalmol Strab 31:123–125
4. Hopkins DJ, Horan EC (1970) Glaucoma in the Hallermann-Streiff syndrome. Br J Ophthalmol 54:416–422
5. Ryan EA, Zwaan J, Chylack LT (1982) Nanophthalmos with uveal effusion. Clinical and embryologic considerations. Ophthalmology 89:1013–1017
6. Wolter JR, Jones DH (1965) Spontaneous cataract absorption in Hallermann-Streiff syndrome. Ophthalmologica 150:401–408

American Journal of Medical Genetics Part A 146A:2162–2163 (2008)

Research Letter

SOX10 Mutation in Waardenburg Syndrome Type II

Manami Iso,[1] Maki Fukami,[1] Reiko Horikawa,[2] Noriyuki Azuma,[3] Nobuko Kawashiro,[4] and Tsutomu Ogata[1]*

[1]Department of Endocrinology and Metabolism, National Research Institute for Child Health and Development, Tokyo, Japan
[2]Division of Endocrinology and Metabolism, National Center for Child Health and Development, Tokyo, Japan
[3]Division of Ophthalmology, National Center for Child Health and Development, Tokyo, Japan
[4]Division of Otorhinolaryngology, National Center for Child Health and Development, Tokyo, Japan

Received 20 February 2008; Accepted 3 May 2008

How to cite this article: Iso M, Fukami M, Horikawa R, Azuma N, Kawashiro N, Ogata T. 2008. *SOX10* mutation in Waardenburg syndrome type II. Am J Med Genet Part A 146A:2162–2163.

To the Editor:

Waardenburg syndrome (WS) is a congenital developmental disorder characterized by sensorineural hearing loss and abnormal pigmentation of the eye, hair, and skin [Jones, 2006]. This condition is divided into four types [reviewed in Jones, 2006; Bondurand et al., 2007]. Type I WS (WS1) consists of dystopia canthorum and broad nasal root, and is almost exclusively caused by heterozygous mutations of *PAX3*. Type II WS (WS2) lacks the dystopia canthorum and results from heterozygous mutations of *MITF* (WS2A) in ~15% of patients and homozygous deletions of *SNAI2* (WS2D) in two patients. Type III WS (WS3) (Klein–Waardenburg syndrome), a severe form of WS1, is associated with upper limb defects, and is ascribed to heterozygous or homozygous mutations of *PAX3*. Type IV WS (WS4) (Shah–Waardenburg syndrome) is characterized by Hirschsprung disease, and is caused by heterozygous or homozygous mutations of *EDNRB* or its ligand *EDN3*, or by heterozygous mutations of *SOX10*.

Thus, the underlying causes remain to be clarified in most of the WS2 patients. While a WS2 locus is mapped to chromosome 1p (WS2B) [Lalwani et al., 1994] and chromosome 8q23 (WS2C) [Selicorni et al., 2002], a causative gene(s) has not been identified from these regions. In this regard, Bondurand et al. [2007] have recently identified *SOX10* deletions in patients with WS2, implying that *SOX10* abnormalities can cause WS2 (WS2E) as well as WS4. Here, we describe another case of WS2E caused by heterozygous *SOX10* mutation.

This Japanese girl was born to nonconsanguineous healthy parents at 41 weeks of gestation after an uncomplicated pregnancy and delivery. At birth, her length was 49.6 cm (+0.6 SD), and her weight 3.4 kg (+0.1 SD). She was found to have light blue eyes, and referred to us at 12 days of age. She manifested hypopigmented irides and a piece of white forelock, but lacked dystopia canthorum, broad nasal root, and Hirschsprung disease. Ophthalmologic examinations revealed bilateral ocular albinism with hypopigmented fundus and hypochromic iris. At 3.5 months of age, auditory brainstem response was performed because of poor responses to sounds, showing bilateral severe sensorineural deafness (hearing level, 90 dB bilaterally). Brain computed tomography showed no abnormal finding. On the basis of the above findings, she was diagnosed as having WS2.

After obtaining written informed consent, direct sequencing was performed for leukocyte genomic DNA of this patient, detecting no abnormality in the coding sequences of *PAX3*, *MITF*, and *SNAI2*. However, we identified a heterozygous *SOX10* frameshift mutation (c.506delC) on exon 4 that is predicted to result in a premature termination at the 284th amino acid (p.Pro169fsX284) (Fig. 1A). The primer sequences and the annealing temperature used were: exon 3, GTTGGACTCTTTGCGAGGAC and ATCCACCCGAAGCTAGAGG (58°C); exon 4, AGCCCCTCTGCTGTCCTCT and CACCCTCAGCTCTGTCATCA (60°C); and exon 5, CTAACCTGCTTCCCCCTTG and CAAGGAACAGGGCACACAG (58°C). This frameshift mutation located within the high mobility group (HMG) DNA-binding domain, and removed the C-terminal part of the HMG domain and the whole transactivation domain. This mutation is predicted to destroy an *Nci*I restriction site, and

*Correspondence to: Tsutomu Ogata, M.D., Department of Endocrinology and Metabolism, National Research Institute for Child Health and Development, Tokyo 157-8535, Japan. E-mail: tomogata@nch.go.jp

Published online 14 July 2008 in Wiley InterScience (www.interscience.wiley.com)
DOI 10.1002/ajmg.a.32405

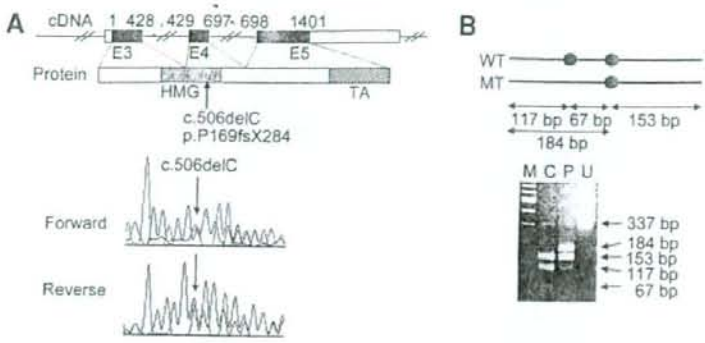

FIG. 1. Mutational analysis of *SOX10*. **A**: Direct sequencing of exon 4. Shown on the upper part is a schematic representation indicating the coding exons 3–5 (E3–E5) and the functional domains. For the *SOX10* cDNA, the black and white areas denote the coding regions and the untranslated regions, respectively, and the Arabic numbers indicate the cDNA sequence encoded by each exon. For the SOX10 protein, the gray and striped squares represent the high mobility group (HMG) DNA-binding domain and the transactivating (TA) domain. Electrochromatograms (forward and reverse) indicate a heterozygous c.506delC mutation on exon 4. **B**: Restriction enzyme analysis. The black circles represent *Nci*I restriction sites. PCR products contain naturally occurring two *Nci*I sites on the wild-type (WT) exon 4, and one of the two *Nci*I sites is predicted to be destroyed on the mutant (MT) exon 4. After *Nci*I digestion, WT sequence specific 117 and 67 bp bands only are found for a control subject (C), whereas WT specific 117 bp and 67 bp bands and a MT specific 184 bp band are shown for the patient (P). M: size marker, and U: undigested PCR product (337 bp).

this was confirmed by the *Nci*I digestion of the corresponding PCR products (Fig. 1B). While the parents postponed the decision to have the genetic testing, this mutation was absent in 100 control subjects.

The results provide further support for the notion that WS2 can be caused by heterozygous abnormalities of *SOX10* (WS2E). In this regard, a *SOX10* frameshift mutation (c.1076–1077delGA, p.Thr360fs X399) has been identified not only in a patient with a typical WS4 but also in the mother with an apparently WS2-compatible deafness and white forelock only phenotype [Pingault et al., 1998]. In addition, another *SOX10* missense mutation (p.Ser135Thr) has also been detected in a patient with "Yemenite deaf-blind hypopigmentation syndrome" mimicking WS2 [Bondurand et al., 1999]. These findings, together with *SOX10* deletions in patients with WS2 [Bondurand et al., 2007], imply that heterozygous *SOX10* abnormalities lead to not only WS4 but also to the WS2 phenotype. Such phenotypic variability would not be unexpected, because it is known that heterozygous mutations of developmental genes are usually associated with wide range of expressivity and penetrance [Fisher and Scambler, 1994]. In addition, the position of the frameshift mutation on exon 4 may also be relevant to the lack of associated features, because *SOX10* mutations residing on the last exon frequently lead to more severe phenotypes such as chronic intestinal pseudo-obstruction and/or neurological features, probably due to escape from the nonsense mediated mRNA decay [Pingault et al., 2000, 2002; Inoue et al., 2004].

REFERENCES

Bondurand N, Kuhlbrodt K, Pingault V, Enderich J, Sajus M, Tommerup N, Warburg M, Hennekam RC, Read AP, Wegner M, Goossens M. 1999. A molecular analysis of the yemenite deaf-blind hypopigmentation syndrome: SOX10 dysfunction causes different neurocristopathies. Hum Mol Genet 8:1785–1789.

Bondurand N, Dastot-Le Moal F, Stanchina L, Collot N, Baral V, Marlin S, Attie-Bitach T, Giurgea I, Skopinski L, Reardon W, Toutain A, Sarda P, Echaieb A, Lackmy-Port-Lis M, Touraine R, Amiel J, Goossens M, Pingault V. 2007. Deletions at the SOX10 gene locus cause Waardenburg syndrome types 2 and 4. Am J Hum Genet 8:1169–1185.

Fisher E, Scambler P. 1994. Human haploinsufficiency—One for sorrow, two for joy. Nat Genet 7:5–7.

Inoue K, Khajavi M, Ohyama T, Hirabayashi S, Wilson J, Reggin JD, Mancias P, Butler IJ, Wilkinson MF, Wegner M, Lupski JR. 2004. Molecular mechanism for distinct neurological phenotypes conveyed by allelic truncating mutations. Nat Genet 36:361–369.

Jones KL. 2006. Waardenburg syndrome, types I and II. In: Jones KL, editor. Smith's recognizable patterns of human malformation. Philadelphia: Elseview Saunders. p 278–279.

Lalwani AK, Baldwin CT, Morell R, Friedman TB, San Agustin TB, Milunsky A, Adair R, Asher JH, Wilcox ER, Farrer LA. 1994. A locus for Waardenburg syndrome type II maps to chromosome 1p13.3–2.1. Am J Hum Genet 55:A14.

Pingault V, Bondurand N, Kuhlbrodt K, Goerich DE, Préhu MO, Puliti A, Herbarth B, Hermans-Borgmeyer I, Legius E, Matthijs G, Amiel J, Lyonnet S, Ceccherini I, Romeo G, Smith JC, Read AP, Wegner M, Goossens M. 1998. SOX10 mutations in patients with Waardenburg-Hirschsprung disease. Nat Genet 18:171–173.

Pingault V, Guiochon-Mantel A, Bondurand N, Faure C, Lacroix C, Lyonnet S, Goossens M, Landrieu P. 2000. Peripheral neuropathy with hypomyelination, chronic intestinal pseudo-obstruction and deafness: A developmental "neural crest syndrome" related to a SOX10 mutation. Ann Neurol 48:671–676.

Pingault V, Girard M, Bondurand N, Dorkins H, Van Maldergem L, Mowat D, Shimotake T, Verma I, Baumann C, Goossens M. 2002. SOX10 mutations in chronic intestinal pseudo-obstruction suggest a complex physiopathological mechanism. Hum Genet 111:198–206.

Selicorni A, Guerneri S, Ratti A, Pizzuti A. 2002. Cytogenetic mapping of a novel locus for type II Waardenburg syndrome. Hum Genet 110:64–67.

黄斑を形成する遺伝子システムと再生医療への応用

Gene mechanism that relates to formation of the fovea and its contribution to reproducing medicine

東　範行
Noriyuki Azuma
国立成育医療センター眼科

◎黄斑は中心視力を得るための高度な網膜構造である．Pax6 はすべての動物における眼形成の master control 遺伝子であるが，ヒトの黄斑低形成で Pax6 遺伝子の変異が発見されたことから，黄斑の形成に関与していると思われる．Pax6 は選択的スプライスのエクソン 5a を含むアイソフォーム Pax6(+5a)と含まない Pax6(−5a)があり，異なる転写因子の働きをもつが，黄斑の形成には Pax6(+5a)がかかわっていることが示唆された．このような黄斑の形成にかかわる遺伝子システムを応用すれば，網膜の再生において高度な視覚を獲得できることが期待される．

Key word：黄斑，形態形成遺伝子，Pax6，選択的スプライス

黄斑は網膜において高度な視覚である中心視力をつかさどるために細胞が密に集中する特殊な部位である．この形成機構には何らかの遺伝子が働いているはずであるが，これまでほとんど検討されていなかった．先天性の黄斑低形成において眼の形成遺伝子 Pax6 の変異がみつかったことが発端になって，この遺伝子の働きが *in vitro*，*in vivo* で検討され，網膜の高度構造をつくるシステムが明らかになりつつある．

眼形成のmaster control遺伝子Pax6

Pax 遺伝子群は paired box と homeobox を共通モチーフとしてもつ遺伝子ファミリーで，422 のアミノ酸をコードする．Pax 蛋白では paired box から翻訳される paired domain がおもに標的遺伝子に結合する(図 1)．この遺伝子群は最初にショウジョウバエで発見され，脊椎動物では 9 種みつかっており，Pax6 はその 6 番目にあたる．ヒトの Pax6 遺伝子は最初に先天無虹彩の原因遺伝子として染色体 11p13 領域の欠失部位から positional cloning によって発見された[1]．

その後，この遺伝子がマウスやラットで変異があると小眼球を起こす small eye(Sey)や，ショウジョウバエで複眼が形成されない eyeless と相同であることが判明した．さらに，ショウジョウバエ初期胚のさまざまな部位にこの遺伝子を導入すると(target expression)，触覚や翅，肢などに異所性に複眼が発生したことから，眼の器官全体をつくる強力な形態形成遺伝子であることが明らかになった[2]．器官の形態形成には全体的に支配する master control 遺伝子があると予測されていたが，下等動物とはいえ，眼というもっとも複雑な器官でその遺伝子がいきなりみつかったのである(図 2)．

その後，さまざまな動物で Pax6 遺伝子がみつかり，脊椎動物，軟体動物の眼や昆虫の複眼だけでなく，プラナリアの原始眼や線虫の光感受性細胞にも存在しており，塩基配列が高度に保存されていたことから，眼の起源に関する考えに大きな転換をもたらした．動物には，種によって複眼，鏡眼，カメラ眼などさまざまな形態の眼があり，従来は 40〜60 系統が別々に発生した(収斂進化)と考えられていた．しかし，Pax6 がすべての動物

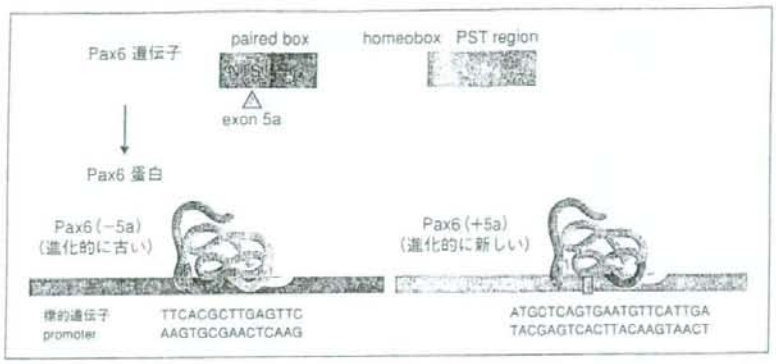

図 1　Pax6遺伝子と蛋白の構造

主要構造として，paired domain(標的 DNA に接触する部位．ここに相当する遺伝子配列を paired box という)，homeodomain(標的 DNA に接触するとともに形態形成遺伝子に特徴的な配列，遺伝子では homeobox)，末尾にプロリン，セリン，スレオニンを多く含む activating domain をもつ．エクソン 5 とエクソン 6 の間に 14 のアミノ酸をコードする選択的スプライスのエクソン 5a があり，2 種類のアイソフォームがつくられる．Paired domain はさらに N-terminal subdomain(NTS)と C-treminal subdomain(CTS)の 2 つに分かれ，標的 DNA が異なる．エクソン 5a による 14 アミノ酸が入れば CTS が，入らなければ NTS が働く．

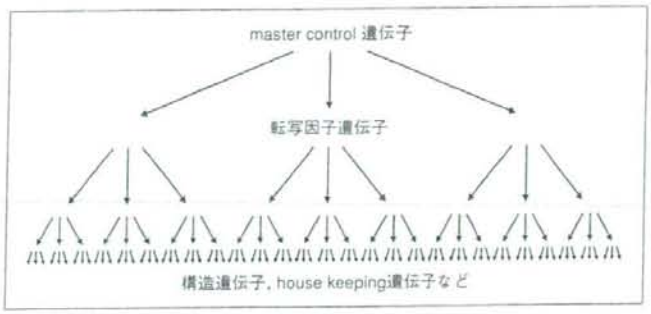

図 2　転写因子遺伝子カスケード

発生において組織ごとに上流遺伝子が下流を支配し，その頂点に器官形成全体を統合する master control 遺伝子が存在する．

の眼に存在することから，眼が原始の祖先動物で光を感じる細胞としてただ一度だけ出現し，進化とともに多彩な形態をとるようになったという単一起源説が支持されるようになった[2]．

Pax6遺伝子の変異によって起こるヒト眼形成異常

In situ hybridization や免疫染色によって Pax6 の発現を検討すると，発生初期は中枢神経や眼原基，中枢神経では前脳，後脳，神経管脳室傍側，下垂体，嗅脳，眼ではまず視溝，ついで眼胞，表面外胚葉と水晶体板，網膜，角膜の順で，眼球ほぼ全体を網羅している(図 3)[3]．以上から，この遺伝子に変異が起こればきわめて多くの先天異常を起こすと推察された．

先天無虹彩では多くの変異が見出されてきたが，そのほかにも Peters 奇形のような前眼部形成不全，角膜ジストロフィー，瞳孔形成異常，先天白内障，黄斑低形成，視神経形成不全で変異がみつかり(図 4)[4-6]，Pax6 がヒトでも前眼部から眼底まで広い範囲で眼の形成を担っていることが分子遺伝学からも証明された．太古に光を感じる細胞